

Coincidence Doppler Broadening of Positron Annihilation Radiation in Fe

E do Nascimento, V R Vanin, N L Maidana and O Helene

Instituto de Física da Universidade de São Paulo, São Paulo, SP, Brasil

eduardon@if.usp.br

Abstract. We measured the Doppler broadening annihilation radiation spectrum in Fe, using $^{22}\text{NaCl}$ as a positron source, and two Ge detectors in coincidence arrangement. The two-dimensional coincidence energy spectrum was fitted using a model function that included positron annihilation with the conduction band and $3d$ electrons, $3s$ and $3p$ electrons, and in-flight positron annihilation. Detectors response functions included backscattering and a combination of Compton and pulse pileup, ballistic deficit and shaping effects. The core electrons annihilation intensity was measured as 16.4(3) %, with almost all the remainder assigned to the less bound electrons. The obtained results are in agreement with published theoretical values.

1. Introduction

Doppler broadening of electron-positron annihilation radiation is an important tool in the field of materials science and has been used since the 1970s in the investigation and characterization of point defects in materials [1,2]. This technique has been applied more recently in intermetallic alloys as prospective materials for new industrial applications [3]. In fact, vacancies and other lattice defects have a significant impact on mechanical as well as electrical properties of materials [3]. As a non-destructive method, upon penetration into the sample, positrons lose almost all of their kinetic energy, reach thermal equilibrium and diffuse into the material before annihilation. During the electron-positron annihilation process, the energy-momentum is conserved and, in most of the cases, two photons are emitted with energies given by $E_{1,2} = m_e c^2 - B_i/2 \pm p_z c/2$, where $m_e c^2$ is the electron rest mass energy, B_i the electron binding energy, c the speed of light, and p_z the momentum component of the electron-positron pair in the direction of the emitted gamma-rays. The use of two Ge detectors allows the observation of both annihilation photons in the Doppler Broadening Spectroscopy [4], with great improvement in the combined energy resolution for the study of the annihilation peak and an important reduction in the observed background, when compared to measurements taken with one detector.

In this paper, we report an experiment of Coincidence Doppler Broadening Spectroscopy (CDBS) of positron annihilation in Fe. A model function was fitted to the obtained data in order to determine the distribution of electron momenta, in a procedure similar to that applied to CDBS for aluminum and silicon [5,6], using core electron binding energies taken from literature [7]. This procedure allows the experimental determination of the annihilation parameters and response function parameters along with their uncertainties.



2. Experimental Setup

A 3.7×10^5 Bq (10 μ Ci) $^{22}\text{NaCl}$ carrier free Amersham positron source was deposited directly between two 2-mm-thick polycrystalline iron discs (99.99% pure) and positioned in the middle of two Ge detectors with end caps standing 10 cm apart, in coincidence arrangement. The detectors were calibrated in energy using the gamma-rays from an ^{192}Ir source placed near the iron discs. A 2D-spectrum was taken for 76 h with about 1.8×10^7 counts in the annihilation photons coincidence peak. The resolutions of the detectors were 1.6 and 1.3 keV for 511 keV photons.

Figure 1 shows the obtained coincidence spectrum. When E_1 and E_2 represent the photons energies measured in the detectors, it is found that the coincidence peak is broader along the line $E_1 + E_2 = 2m_e c^2$ due to the Doppler shift of the annihilation radiation. The ridges crossing below the annihilation peak are due to coincidences with annihilation photons or 1274 keV gamma-rays from ^{22}Na decay that undergo Compton scattering inside the detector active volume. The spectrum also shows features that cannot be seen in this figure [8]: exponential tails due to ballistic deficit, pulse shaping problems, pileup, and events of backscattering of the annihilation photons. There is still a small fraction of positrons that annihilate before thermalizing, the so-called *in-flight positron annihilation*, and the corresponding events show a larger energy spread, of a few hundreds of keV. It is also seen in Figure 1 a continuum between the ridges, associated to events where both photons scatter in the detectors and escape the active volumes. There is more information in this spectrum, that cannot be retrieved by visual inspection as, for example, the various distributions related to annihilation with core electrons from different shells, which are displaced from the line $E_1 + E_2 = 2m_e c^2$ by their binding energies B_i . Accidental coincidences were corrected using another matrix built with the time window displaced from the prompt peak.

3. Fitting – Function Model

A two dimensional function was fitted to the experimental histogram (Figure 1) in a 90 keV \times 90 keV region around the two annihilation-photons coincidence peak. The main components of this model function are described below.

Positron annihilation with electrons of the conduction band was represented by:

$$f_c = \sum_{i=1}^3 C_i (E_1 - E_2 - \alpha_i) (E_1 - E_2 + \alpha_i) \quad (1)$$

along the line $E_1 + E_2 = 1022$ keV, where α_i are the cutoff parameters ($C_i = 0$ when $|E_1 - E_2| > \alpha_i$). We fitted the empirical parameters C_i and α_i to the experimental spectrum. The $3d$ orbital was included in these terms because the detector resolutions did not allow to separate this orbital from the conduction band; hence, we have defined an effective band of less bound electrons, in a procedure similar to that adopted by Tang [8]. Eventually, this term will include also the contribution from the electrons within the defects.

Positron annihilation with core electrons was described by Gaussian functions:

$$f_{nl} = \frac{A_{nl} e^{-(E_1 - E_2)^2 / 2\sigma_{nl}^2}}{\sqrt{2\pi}\sigma_{nl}} \quad (2)$$

along the line $E_1 + E_2 + B_{nl} = 1022$ keV, where B_{nl} is the nl -orbital binding energy [7]; here, nl stands for $3s$ and $3p$. We fitted the empirical parameters A_{nl} and σ_{nl} .

The in-flight positron annihilation was taken into account by a function that depends on the angle θ between the emitted annihilation photons,

$$f_f = A_f e^{-\lambda/d(\theta)} \quad (3)$$

where the constraint equation $d(\theta) = E_1^{-1} + E_2^{-1} = (1 - \cos\theta)/m_e c^2$ comes from the conservation laws [6], and relation (3) extends over all $E_{1,2}$ consistent with this constraint. Here we fitted the empirical parameters A_f and λ .

Finally, spectrum distortion by the ballistic deficit, pulse pileup, and incomplete charge collection were taken into account using internal ($E_{1,2} < m_e c^2$) and external ($E_{1,2} > m_e c^2$) exponential tails for each detector. The two internal and two external ridges were included in the model function to account for coincidence events where one of the annihilation photons is measured in the full energy peak and the other undergoes scattering in the detector before escaping the active volume. It was assumed that the continuum is proportional to the ridges and, thus, the only fitted parameter is the proportionality factor [5,6]. We fitted also the coincidence peak two-dimensional position, the inclination of the $E_1 + E_2 = 2m_e c^2$ line with respect to the CDBS axes, and two parameters for the detector resolutions.

The functions f_c , f_{nb} , f_f , the exponential tails, the ridges, and the background were added and convolved with the detector response functions given by two Gaussians. The fitted spectrum is shown in figure 2. The chi-squared value (χ^2) was calculated using the expression:

$$\chi^2 = \sum_{i,j} \frac{(n_{ij} - F_{ij})^2}{F_{ij} + 2a_{ij}} \quad (4)$$

where n_{ij} is the number of observed events in channel (i,j) of the Doppler broadening real coincidence spectrum, a_{ij} is the number of observed events in channel (i,j) of the Doppler broadening accidental coincidence spectrum and F_{ij} is the fitted function.

4. Results and Conclusion

With this simplified model, the obtained χ^2 value was 3.98×10^4 for about 3.06×10^4 degrees of freedom. This chi-squared value corresponds to a low significance level, and shows that this simple model is unable to explain the phenomenon in its complexity.

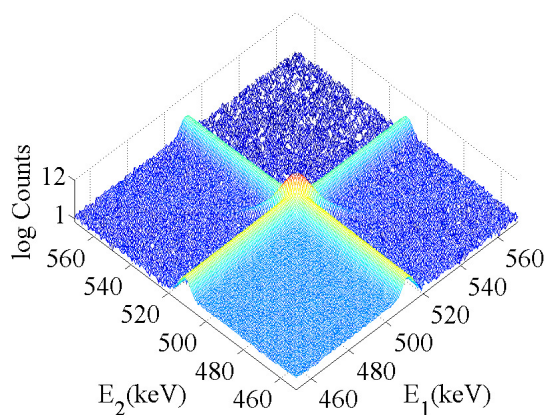


Figure 1. Experimental coincidence Doppler Broadening spectrum of the annihilation radiation in Fe.

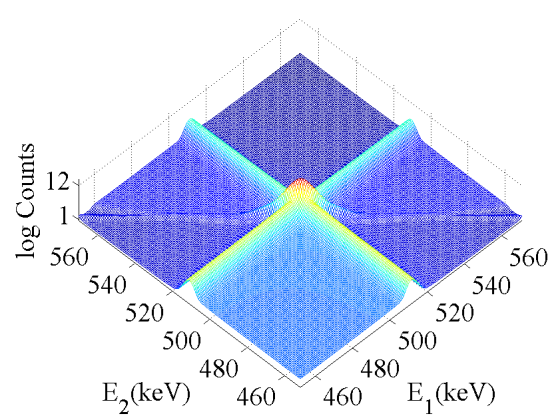


Figure 2. Fitted coincidence Doppler Broadening spectrum of the annihilation radiation in Fe.

Figure 3 shows the fitted and experimental Doppler broadening profile spectrum for Fe, where the $3p$ plus $3s$ electrons correspond to 16.4 (3) % of total annihilation events, with the remaining

83.6 (3) % assigned to conduction, 3d electrons, and defects; these intensities can be compared to those calculated by Tang et al. [9], respectively $\sim 15.6\%$ and $\sim 84.4\%$. In-flight positron annihilation amounts to a small fraction of percent, and the corresponding events are shown along with backscattering events in Fig. 2. The less bound electron band (conduction, 3d, and defects) cutoff parameters obtained were $7, 12$ and $17 \times 10^{-3} m_e c$. We call attention for the fact that our Fe sample was polycrystalline, therefore the measurement corresponds to an average of the orientations of the momentum distributions of electrons in the sample.

In conclusion, with the simplified model presented here – three parabolas and two Gaussian functions with a standard response function [5,6] – we were able to describe the main components of the electron-positron annihilation peak in Fe, as can be seen in Figure 3, and obtained annihilation intensities in agreement with theoretical results. Thus, it could be possible to identify the chemical element present in the annihilation site by CDBS experiment, with relatively few counts.

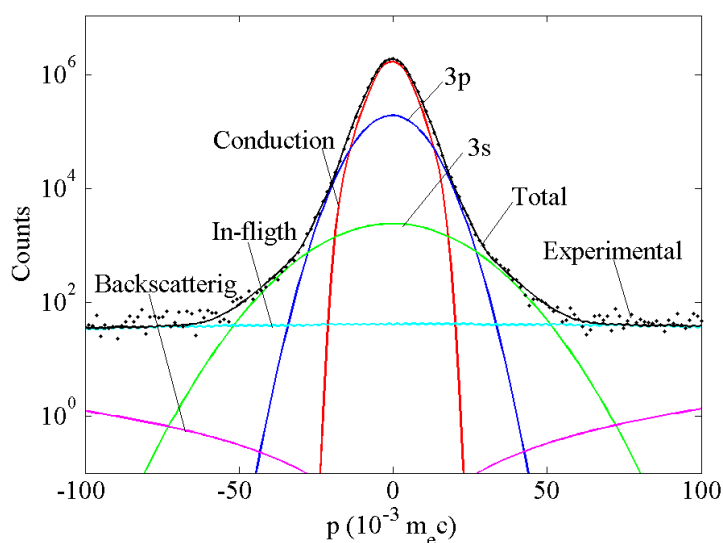


Figure 3. Fitted and experimental Doppler broadening profile spectrum for Fe, including the 3p, 3s and conduction electrons components of annihilation events. In-flight positron annihilation and backscattering events in the same region of interest are also shown.

Acknowledgments

We acknowledge the support of Conselho Nacional de Desenvolvimento Científico e Tecnológico – CNPq, Coordenação de Aperfeiçoamento de Pessoal de Nível Superior – CAPES and Fundação de Amparo à Pesquisa do Estado de São Paulo – FAPESP.

References

- [1] Krause-Rehberg R and Leipner H 1999 *Positron Annihilation in Semiconductors* (Springer-Verlag, Berlin)
- [2] Puska M J and Nieminen R M 1994 *Reviews of Modern Physics* **66** 841
- [3] Melikhova O, Cizek J, Kuriplach J, Prochazka I, Cieslar M, Anwand W and Brauer G 2010 *Intermetallics* **18** 592
- [4] Lynn K G, MacDonald J R, Boie R A, Feldman L C, Gabbe J D, Robbins M F, Bonderup E and Golovchenko J 1977 *Phys Rev Lett* **38** 241
- [5] do Nascimento E, Helene O, Vanin V R and Takiya C 2005 *Nucl Instrum Meth A* **538** 723
- [6] do Nascimento E, Helene O, Vanin V R, da Cruz M T F and Morales M 2009 *Nucl Instrum Meth A* **609** 244
- [7] Firestone R B and Shirley V S 1996 *Table of Isotopes*, eighth edition, vol II, John Wiley & Son
- [8] do Nascimento E, Fernández-Varea J M, Vanin V R, Helene O and Maidana N L 2011 *AIP Conf Proc* **1351** 216
- [9] Tang Z, Hasegawa M, Nagai Y and Saito M 2002 *Phys Rev B* **65** 195108-1